

---

# C-FAR: a Clustering ensemble method with Fast, Automated and Reproducible assessment applied to longitudinal neural tracking

---

Hanlin Zhu<sup>1</sup> Xue Li<sup>1</sup> Liuyang Sun<sup>1</sup> Fei He<sup>1</sup> Zhengtuo Zhao<sup>1</sup> Lan Luan<sup>1</sup> Ngoc Mai Tran<sup>2</sup> Chong Xie<sup>1</sup>

## Abstract

Across many areas, from neural tracking to database entity resolution, manual assessment of clusters by human experts presents a bottleneck in rapid development of scalable and specialized clustering methods. To solve this problem we develop C-FAR, a novel method for Fast, Automated and Reproducible assessment of multiple hierarchical clustering algorithms simultaneously. Our algorithm takes any number of hierarchical clustering trees as input, then strategically queries pairs for human feedback, and outputs an optimal clustering among those nominated by these trees. While it is applicable to large dataset in any domain that utilizes pairwise comparisons for assessment, our flagship application is the cluster aggregation step in spike-sorting, the task of assigning waveforms (spikes) in recordings to neurons. On simulated data of 96 neurons under adverse conditions, including drifting and 25% blackout, our algorithm produces near-perfect tracking relative to the ground truth. Our runtime scales linearly in the number of input trees, making it a competitive computational tool. These results indicate that C-FAR is highly suitable as a model selection and assessment tool in clustering tasks.

## 1. Introduction

Over the past three decades, intensive research on developing novel clustering algorithms have resulted in a plethora of choices. However, in many applications, model selection is an arduous task performed by human experts: one needs to assess the quality of clusters through pairwise comparisons, then manually tune the algorithms' parameters. This is time consuming, subjective, and clearly do not scale. This presents a fundamental roadblock in efficient processing of massive datasets. This problem is common to text classification (Schütze et al., 2006), entity resolution in databases (Wang et al., 2012; Vesdapunt et al., 2014; Gokhale et al., 2014; Mazumdar & Saha, 2017b), biomedical problems (Wiwie et al., 2015) and a wide variety of crowd-sourcing tasks (Mazumdar & Saha, 2017a). The flagship example that

ignited this project stems from spike sorting in neuroscience. This is the problem of assigning waveforms (spikes) to neurons, the first and fundamental step in processing neural data from electrode arrays. For *in vivo* recordings, neurons can only be indirectly identified as a cluster of similar waveforms. Continuous improvements over electrode designs (Blanche et al., 2005; Chung et al., 2019; Hong & Lieber, 2019) now enable almost continuous *in vivo* recordings of over 100 electrodes over a month, producing *half a terabyte of data* per day per animal. Over such a large time span, the target neurons may undergo biological or positional changes over a day or a week (Rousche & Normann, 1992; Szarowski et al., 2003; Subbaroyan et al., 2005; Gilletti & Muthuswamy, 2006; Barrese et al., 2013), resulting in a different waveform. Existing spike-sorting algorithms (Takahashi et al., 2002; Takekawa et al., 2012; Carlson et al., 2013; Rodriguez & Laio, 2014; Rossant et al., 2016; Chung et al., 2017; Song et al., 2018) were developed under the assumption that a neuron's average waveform is constant, and thus are not effective for long, continuous recordings. In practice, automated spike sorting is performed on binned segments of 30 to 60 minutes, then the units in different time bins are aggregated using clustering algorithms such as mutual nearest neighbors (mNNs) between adjacent bins (Chung et al., 2019). However, a neuron may not be active at all hours due to the subject's behavior, waveform drifting, or intermittent electrode failures. This results in many more waveform clusters than there could be neurons in the recording range (cf. Figure 2). Though different clustering metrics and algorithms could be applied, after their applications, experts still need to spend hours to curate the results. Effectively, they are doing a manual assessment and selection of different clustering models' outputs using pairwise comparisons.

## 2. Our contributions

This project develops and implements C-FAR, a novel method for **fast, automated and reproducible** assessment of multiple hierarchical clustering algorithms simultaneously. Our algorithm takes any number of hierarchical clustering trees as input, then strategically queries pairs for human feedback, and outputs a provably optimal par-

tition of the data among those nominated by the various input trees, along with a summary of the trees' contributions and deviations. Our approach builds on the recent work in (Gentile et al., 2019), which partitions the data by trimming a hierarchical clustering tree  $T$  using pairwise comparisons. We generalize the binary search of (Gentile et al., 2019) to an efficient and recursive algorithm to find the optimal partition across multiple trees. The core idea is illustrated in Figure 4.

Rather than being “yet another clustering algorithm”, C-FAR can be deployed to assess and improve any collection of hierarchical clustering methods. Unlike existing cluster assessment techniques (Seo & Shneiderman, 2002; Nam et al., 2007; Schreck et al., 2009; Lex et al., 2010; Cavallo & Demiralp, 2018) which mainly focus on visualizing different algorithms' outputs but otherwise let the user freely explore or reassign clusters, our algorithm requires the user to answer a set of queries strategically chosen by the algorithm, and thus is completely reproducible.

Using MEArec (Buccino & Einevoll, 2019), we simulated a dataset of 96 neurons of two different types, with biophysically plausible drifts and waveforms. For each combination of parameters (number of trees and dropout rate), we simulated 100 trials and chose  $m \in \{1, 2, 4, 8, 32, 120\}$  random trees out of a set of 120 hierarchical clustering trees obtained by varying different parameters such as distance metric and linkage type (see Section 4.1 for details). Figure 1 shows the performance statistics of C-FAR averaged over 100 such trials. The C-FAR algorithm performs well even under adverse conditions and the runtime scales linearly in the number of input trees, making it a competitive computational tool.

## 2.1. Contributions to the spike-sorting literature

Most spike sorting algorithms start with a dimension reduction step such as principal component analysis (PCA), followed by a clustering step. There is a large methodology literature that builds on a combination of many techniques: independent component analysis (Takahashi et al., 2002), Kalman filter (Calabrese & Paninski, 2011), variational Bayes (Takekawa et al., 2012), mixture modeling (Carlson et al., 2013), peak-density (Rodriguez & Laio, 2014), singular value decomposition (Pachitariu et al., 2016), template matching (Yger et al., 2016), random projections (Chung et al., 2017), integer programming (Dhawale et al., 2017), convolutional dictionary learning (Song et al., 2018) and deep neural networks (Li et al., 2019), to name a few. A number of these methods are parametric, and thus can be generalized to allow time-varying features.

However, given the plethora of choices, the bottleneck in fact lies in assessing their results. Even over the short time frame of several hours, automated spike sorting is very difficult due to a complex noise distribution, non-Gaussian

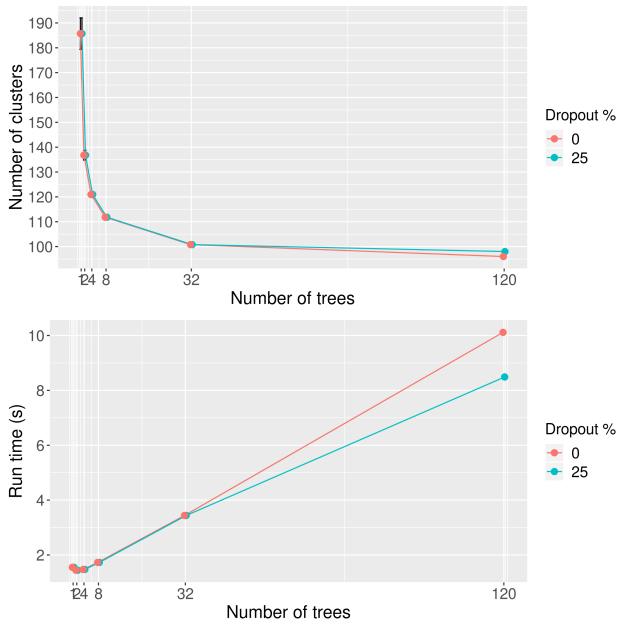


Figure 1. The C-FAR algorithm performs well even under adverse conditions and the runtime scales linearly in the number of input trees, making it a competitive computational tool. **Top.** Mean number of clusters by C-FAR vs number of input trees under two different experimental conditions: no dropout (red) vs 25% dropout rate, meaning that each waveform has a 25% chance of not registering in each timebin (green). The true number of clusters is 96. **Bottom.** Average runtime of C-FAR in seconds vs the number of input trees. In both plots, standard error bars are shown in black. The algorithm shows stable performances even with high dropout rates and near-perfect recovery of the clusters for 32 random trees.

clusters and the presence of biological irregularities such as bursting (Harris et al., 2001; Quirk et al., 2001). All but a few of the above methods still require hours of manual curation (Chung et al., 2017). For longitudinal sorting, the dependency on human experts is only amplified. Direct observation of a neuron is costly, requires special equipment, and can only monitor one neuron at a time (Yger et al., 2018). In practice, clusters are still assessed by experts through pairwise comparisons, with *ad hoc* reassignments and minimal justifications. Instead of yet-another-algorithm, C-FAR supplies the neuroscience community with a fast and reproducible way to assess the quality of multiple clustering methods.

## 2.2. Contributions to the clustering literature

Our proposed C-FAR algorithm functions as a fast algorithm for clustering, as well as a diagnostic tool for comparisons of different hierarchical clustering outputs and an automated model selection method. It straddles across multiple literatures; each offers solutions to one of the above problems

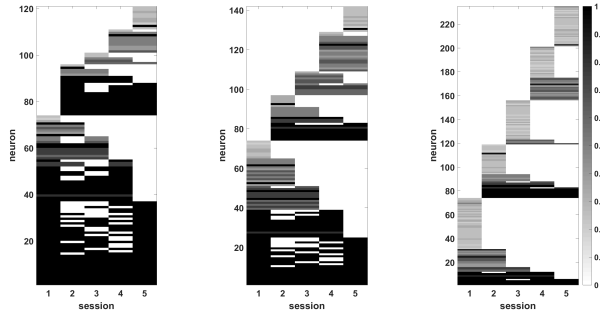


Figure 2. On simulated neuroscience data with biophysically plausible parameters, C-FAR (left) is better than both the single-tree algorithm of (Gentile et al., 2019) (middle) and the automated flattening comparable to clustering methods currently employed in the neuroscience community (Chung et al., 2019) (right). The dataset has 96 neurons, simulated for 5 sessions. Each neuron for each session has a 25% dropout chance. C-FAR was applied with 8 randomly chosen hierarchical clustering trees as input out of 120 trees built with different parameter choices (cf. Section 4.1). The algorithm of (Gentile et al., 2019) was applied to a random chosen tree out of these 120. Automated flattening (with no pairwise comparisons) was computed on this same tree such that each cluster has an average correlation of at least 0.96 between waveforms. For each plot, each row is a cluster corresponding to a putative neuron recovered from the respective method. The x-axis marks the sessions where the waveforms in this cluster appeared. The grayscale color of each cluster shows the recovery rate, defined as the number of sessions of this cluster divided by the number of sessions that the true neuron corresponding to the this cluster appeared in the dataset. Darker color indicates higher recovery rate. Black is 100%, meaning all waveforms of this neuron are perfectly clustered. C-FAR produced 120 clusters, with 78% neurons having 100% recovery rate. The other two methods produced rather more fragmented clusters: (Gentile et al., 2019) produced 140 units while automated flattening produced 224 units, and their perfect recovery rates are lower, at 55% and 26%, respectively. The distribution of recovery rates for each method is shown in the opposite column.

but not all at once.

A number of papers have considered clustering algorithms that minimize number of pair comparisons. Unfortunately, existing algorithms either require unrealistic assumptions such as noise-free comparisons and tight clusters (Eriksson et al., 2011), are specific to a particular clustering algorithm (Shamir & Tishby, 2011; Wauthier et al., 2012; Ailon et al., 2017; Ashtiani et al., 2016; Chatziafratis et al., 2018), or are slow, too general and do not take advantage of existing information offered by the input clustering methods (Dasarathy et al., 2015; Mazumdar & Saha, 2017a; Chen et al., 2014; Krishnamurthy et al., 2012). On the other extreme, ensemble clustering methods aggregate multiple clustering outputs to compute a new partition (Vega-Pons & Ruiz-Shulcloper,

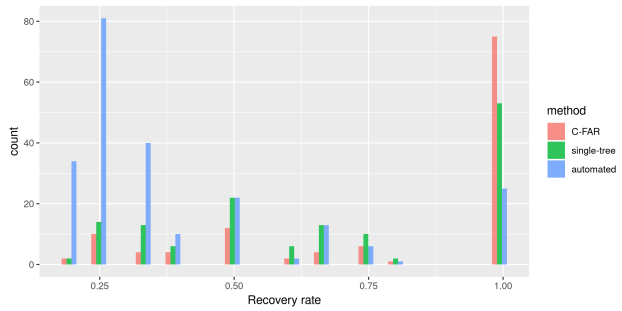


Figure 3. Histogram of recovery rate, accompanies Figure 2.

2011; Alqurashi & Wang, 2019; Fred & Jain, 2005; Strehl & Ghosh, 2002; Karypis & Kumar, 1998; Fern & Brodley, 2004; Iam-On et al., 2011; Mimaroglu & Aksehirli, 2011; Huang et al., 2015; Ayad & Kamel, 2010; Dudoit & Fridlyand, 2003; Fern & Brodley, 2003; Gionis et al., 2007). There are many alternative approaches; among them, object co-occurrence uses pairwise comparisons induced by the different clusters to produce a similarity matrix from which the final partition is computed (Monti et al., 2003; Strehl & Ghosh, 2002; Fred & Jain, 2005). Most methods do not take advantage of cluster similarity measures coming from a hierarchical clustering and thus are often slow, with quadratic complexity in the number of clusters. Critically, unlike our proposed method, user feedback is not taken into account in the construction of the similarity matrix, thus a separate model selection step is required as with any other clustering algorithms.

The difficulty of comparing different clustering methods is common to many applications, most notably in genetics. A variety of methods have been developed to visually compare multiple clustering algorithms (Cao et al., 2011; Lex et al., 2012; L'Yi et al., 2015; Pilhöfer et al., 2012; Zhou et al., 2009; Sacha et al., 2017). A number of these are interactive and allow the user to reassign clusters, supervise a chosen clustering algorithm, or give weights to selected observations (Seo & Shneiderman, 2002; Nam et al., 2007; Schreck et al., 2009; Lex et al., 2010; Cavallo & Demiralp, 2018; Balcan & Blum, 2008; Awasthi et al., 2017). However, the sheer volume of data makes these methods time-consuming to use for neural tracking. More importantly, they often lack reproducibility since users have too much freedom in selecting the type of feedback to give, and not all of the user's decisions are systematically recorded. Furthermore, analyzing the feedback can itself be a complex task, since it can be unclear which decisions are the most consequential in shaping the final partition.

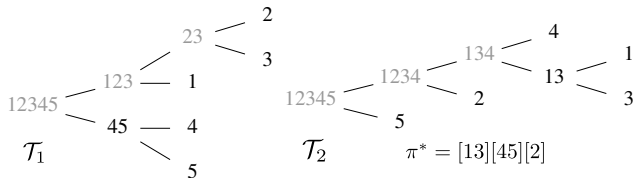


Figure 4. Core idea of C-FAR on a simple example with  $n = 5$  observations. The true partition  $\pi^*$  induces a purity process on each hierarchical clustering tree, where a node is pure (black) if observations in the corresponding partition come from the same true cluster. The purity of a given node can be determined from pairwise comparisons between the leaves of its left and right children. Purity satisfies important inequalities imposed by set inclusion, making it monotone along the branches and allow information to be pooled across trees. For example, if the queries show that  $y(23) = 0$  in tree  $\mathcal{T}_1$ , then  $y(1234) = 0$  in tree  $\mathcal{T}_2$ , and all of their ancestors are also not pure. Our algorithm leverages this fact to search over all trees at once using the same set of pairwise comparisons. It is a fast and recursive way to compute  $\pi^*$ , with provable accuracy and complexity.

### 2.3. Relation to clustering with active learning

Assessing clusters’ qualities by pairwise comparisons is close to active learning, where a learner is given access to unlabeled data and is allowed to adaptively choose which ones to label (Lewis & Gale, 1994). Both share the difficulty of finding a representative sample (Xu et al., 2003), however, cluster assessment has the added difficulty that our search space is over  $\binom{n}{2}$  pairs instead of  $n$  observations (Xiong et al., 2016). Uniform sampling is generally inefficient (Eriksson et al., 2011).

To see this, suppose that data consist of  $k$  clusters generated by independently assigning the label 1 to  $k$  to each observation. Suppose that a partition  $\pi$  that is incorrect on  $p$  fraction in each cluster. Now consider a randomly chosen pair of observations  $(u, v)$ . The probability that they belong to different true clusters and are wrongly put together by  $\pi$  is  $O(p/k)$ . The probability that they belong to the same true cluster and are wrongly separated by  $\pi$  is also  $O(p/k)$ . Thus overall, the probability that  $\pi$  makes a mistake on a randomly chosen pair  $(u, v)$  is  $O(p/k)$ . In particular, if the number of clusters  $k$  is large, as often the case in applications, then uniform sampling is a bad strategy to uncover misclustered pairs.

One may be tempted to sample pairs closer to the boundary of adjacent clusters. For  $k = 2$ , this strategy was the default in the early days of active learning (Lewis & Gale, 1994; Campbell et al., 2000; Tong & Chang, 2001; Xu et al., 2003), but was later shown to induce a serious sampling bias (Dasgupta & Hsu, 2008). Ideally, one would like to sample within clusters to measure purity, sample between clusters to measure modularity, then sample on the boundary for misclassification. A number of papers on active clustering

are built on this intuition (Huang & Lam, 2007; Mallapragada et al., 2008; Wang et al., 2011; Hofmann & Buhmann, 1998). Tractable models for theoretical analysis often assume a specific clustering model and advocate for selecting the most ‘informative’ pair, or one that minimizes empirical uncertainty (Nguyen & Smeulders, 2004; Dasgupta & Hsu, 2008). Some papers view the pairwise comparisons as must-link or must-not-link constraints, then adapt each existing clustering algorithm such as  $k$ -means or spectral clustering into one that would respect these constraints (Xiong et al., 2012; Voiron et al., 2016; Xiong et al., 2016; Lipor & Balzano, 2017). These approaches produce samples highly adapted to a single clustering method, which may not be suitable for assessing another. In other words, they do not advert the key difficulty: how to produce a representative sample that allows fair comparisons between methods?

## 3. Main results

Our work generalizes the recent approach by (Gentile et al., 2019), who used active learning with pairwise comparisons to create partitions from one hierarchical clustering tree. We introduce the concept of node purity, and note that this satisfies important inequalities imposed by the lattice of subsets of  $[n]$  ordered by inclusion. This allows us to generalize the binary search idea that drives the algorithms of (Gentile et al., 2019). As a result, our algorithm can take multiple trees as input, and utilize the same set of pairwise comparisons to simultaneously trim all the trees at once to arrive at the optimal partition. We expect our algorithm to have the same fast performance as that theoretically guaranteed in (Gentile et al., 2019), and this is supported by experiments (cf. Figure 1). First we briefly review the results of (Gentile et al., 2019) before stating our general setup and algorithms.

### 3.1. Partition from one tree by pairwise comparisons

Let  $T = (V, E)$  be a binary tree obtained from applying a hierarchical clustering procedure on some dataset with  $n$  observations. A feedback matrix  $\Sigma \in \{\pm 1\}^{n \times n}$  is a symmetric matrix encoding the binary relations between the observations:  $\Sigma_{ij} = 1$  if observations  $i$  and  $j$  are similar, and  $\Sigma_{ij} = -1$  if they are not. Given  $T$ , an active learning algorithm proceeds in a sequence of rounds. At round  $t$ , the algorithm chooses a pair  $(i, j) \in [n] \times [n]$ , and observes the associated label  $\Sigma_{ij}$ . At some point, the algorithm is stopped, and is compelled to produce a partition of  $[n]$  by selecting a collection of nodes in  $V$  that corresponds to mutually disjoint subsets. The goal is to return a good partition from  $T$  by making as few queries on  $\Sigma$  as possible. We shall assume that there is a ground-truth feedback matrix  $\Sigma^* \in \{\pm 1\}^{n \times n}$  induced by some true partition  $\pi^*$  of  $[n]$ , where  $\Sigma^*_{ij} = 1$  if and only if  $i$  and  $j$  belongs to the same block of  $\pi^*$ . In the noise-free case,  $\Sigma = \Sigma^*$ . In the noisy

case,  $\Sigma$  is obtained from  $\Sigma^*$  by switching the sign of  $\lambda \binom{n}{2}$  entries for some  $\lambda \in (0, 1)$ . Say that  $\pi^*$  is realizable by  $T$  if each of its blocks corresponds to a node of  $V$ .

The key observation of (Gentile et al., 2019) is that if  $\pi^*$  is realizable by  $T$ , then it can be recovered by performing a binary search on paths that connect the root to the leaves. Indeed, let  $y : 2^{[n]} \rightarrow \{0, 1\}$  be the purity function defined on subsets of the data, where  $y(S) = 1$  if all observations in  $S$  belong to the same block of  $\pi^*$ , and 0 else. We can define  $y$  on the nodes of  $T$  by identifying them with the subset of observations that they represent. Since the clusters are hierarchical, for any leaf  $\ell \in T$ , the unique path from the root to  $\ell$  has monotone label: if  $v$  is pure, then any child of it is pure; if  $v$  is not pure, then any parent of it is also not pure (cf. Figure 4). Now, purity of a node  $v$  can be decided by pairwise comparisons of elements from its left and right children. In the noiseless case, one comparison will suffice. In the noisy case, one can do repeated sampling and take majority. Thus one can find the largest pure node along any a given path via binary search, and such a node must be a block of  $\pi^*$  by the realizability assumption. The algorithms in (Gentile et al., 2019) select paths with maximum entropy at each step, do a binary search to find a new block of  $\pi^*$ , update the tree and repeat accordingly.

### 3.2. Best partition from multiple trees with the same set of comparisons

We generalize the above approach to multiple trees as follows. Suppose there are multiple hierarchical clustering methods, which give yield to multiple trees  $\mathcal{T} = \{T_1, T_2, \dots, T_r\}$ . Say that the setup is realizable if each block of  $\pi^*$  correspond to a node in one of the trees in  $\mathcal{T}$ . Let  $y$  be the purity process as above. That is, for a node  $v_i$  in tree  $T_i$ ,  $y(v_i) = 1$  if the cluster corresponding to  $v$  is a subset of a block of  $\pi^*$ , and 0 else. Now,  $y$  satisfies important inequalities imposed by the lattice of subsets of  $[n]$  ordered by inclusion. Namely, for any two subsets  $v_i, v_j$  of the data,

$$\begin{aligned} y(v_i \cap v_j) &\geq \max(y(v_i), y(v_j)), \\ \text{and } y(v_i \cup v_j) &= \min(y(v_i), y(v_j)). \end{aligned} \quad (1)$$

These constraints generalize the key observation of (Gentile et al., 2019) that purity is a monotone non-decreasing process along any branch of a hierarchical clustering tree. When there are multiple trees, (1) enables one to pool information on node purity across multiple trees. This suggests the following algorithm to find one block of the optimal partition. It generalizes the binary search of (Gentile et al., 2019).

**Example 1.** Let the two trees depicted in Figure 4 be input to Algorithm 1. In line 1, we can choose  $S = \{3\}$ . Then  $v_1 = \{2, 3\}$  and  $v_2 = \{1, 3\}$ . Since  $y(\{1, 3\}) = 1$ , we can

---

#### Algorithm 1 FindOneBlock

---

**Input:** hierarchical clustering trees  $\mathcal{T} = \{T_1, T_2, \dots, T_r\}$  on  $[n]$ .

**Output:** one node among the trees  $\mathcal{T}$  which corresponds to one cluster best compatible with the pairwise feedback

---

- 1: Start with a set  $S \subset [n]$ , maximal w.r.t inclusion, which has different minimal extensions  $v_1, v_2, \dots, v_r$  in the  $r$  trees.
  - 2: Determine the purity of  $v_1, \dots, v_r$  by sampling from  $v_1 \setminus S, \dots, v_r \setminus S$ .
  - 3: Renumber so  $\{v_1, \dots, v_m\}$  is the set of pure nodes
  - 4: **if**  $m = 1$  **then**
  - 5:   Do binary search up the tree  $T_1$  on this branch until we find the largest node  $B$  (by inclusion) with purity 1
  - 6: **else**
  - 7:   Look for the minimal extensions  $w_1, \dots, w_r$  of  $S' := v_1 \cup \dots \cup v_m$  in each tree.
  - 8:   Repeat line 2 with  $(v_1, \dots, v_r) := (w_1, \dots, w_r)$  and  $S := S'$ .
  - 9: **end if**
  - 10: **return** the node  $B$
- 

conclude that  $y(23) = 0$ , so  $m = 1$ . Algorithm 1 will then do a binary search along the branch 12345–1234–134–13, find that  $B = \{1, 13\}$ , and output this block of  $\pi^*$ .

**Proposition 1.** *In the noiseless case, if  $\pi^*$  is realizable, then Algorithm 1 outputs one block of  $\pi^*$ .*

*Proof sketch.* Since  $\pi^*$  is realizable by  $\mathcal{T}$ , the initial set  $S$  must have  $y(S) = 1$  and at least one of the  $v_1, \dots, v_r$  must be pure, by minimality, so  $m \geq 1$ . At each iteration, the algorithm produces another pure set  $S'$ , and thus the same argument applies. Repeating this argument shows that the algorithm terminates with finding one block of  $\pi^*$ . Induction on the number of remaining blocks of  $\pi^*$  concludes the proof.  $\square$

## 4. Experimental results

### 4.1. Data simulation and choice of parameters

While the C-FAR algorithm could still perform well in more adverse settings, we have taken care to simulate datasets with biologically plausible parameters. In particular, drifting waveform templates of extracellularly recorded neurons were simulated using MEArec (Buccino & Einevoll, 2019). Modeling the probes reported in (Zhao et al., 2017), we simulated 32 channels recording electrodes arranged into a 2D array of shape  $4 \times 8$  with an electrode center to center distance of  $50 \mu\text{m}$ . Two types of rats somatosensory cortex neuron models included in the paper (Buccino & Einevoll,

2019) (Ramaswamy et al., 2015) were selected : bitufted cells (BTC) and double bouquet cells (DBC). For each of the two neuron types, 48 neuron instances were initially randomly positioned within the area of  $92,400\mu\text{m}^2$  covered by the 2D electrode array. Similar to (Hurwitz et al., 2019), an overhang detection range, in our case  $35\mu\text{m}$ , was allowed to account for the detectable neurons that reside/drift slightly beyond the electrode 2D boundary. Assuming the same overhang, one of the latest in-vivo high density flexible electrodes (Chung et al., 2019) reported an average of  $\sim 16$  neurons (max 45) detected in an array area of  $23320\mu\text{m}^2$ . Assuming that neuron number directly scales with recording area, we would get an average of 63 (max 178) neurons. Therefore, our chosen number of 96 neurons is well within this range. The vertical distance (height) of neuron were bounded within  $10\mu\text{m}$  to  $80\mu\text{m}$  relative to the electrode plane. So far, unanimous opinion or evidence on how fast or in which directions neurons might drift or migrate with respect to the recording electrodes is not present. For some electrode arrays, no preferred moving directions could be observed (Luan et al., 2017) for a few weeks during which neurons moved  $\sim 10\mu\text{m}$ . For other electrode designs, neurons could move as far as  $20\mu\text{m}$  mostly along vertical directions (Pachitariu et al., 2018) in a single experiment session. For our simulation, the 96 neurons were simulated to move with a given constant velocity for 5 steps resulted in a total of 480 detected units, analogous to 480 spike-sorted neurons detected across a total of 5 intermittent in-vivo recording sessions. With drifting magnitude of at least  $7\mu\text{m}$  per step, the number of possible drifting directions were limited to a maximum of 5 per type of neuron. To further increase the difficulty of the task, physiologically feasible random rotations were applied at each time step as described in (Buccino & Einevoll, 2019). Finally, in reality, the number of activated and detectable neurons at any given time step are affect by numerous factors such as the behavioral state of the animal (Blanche et al., 2005). To simulate random inactivation of neurons, in a separate dataset, a 25 % drop out chance was applied to the 96 neurons at each of the 5 drifting steps, meaning that the waveform for this neuron is missing for this step. This resulted in a total of 360 detected units. Recorded waveforms on any channel was down-sampled to have 38 time points. Therefore, the waveform of each of 480 or 360 units was represented as a 3D array of shape  $4 \times 8 \times 38$ , which was later spatially flattened into  $1 \times 1216$  array. A list of labels indicating which of the 96 seed neurons that the 480 or 360 units correspond to was also generated to serve as the ground truth.

## 4.2. Creating the original hierarchical clustering ensemble

Agglomerative hierarchical cluster trees were created with the original MATLAB function `linkage()` based on the

pairwise waveform distance of the input units. By varying parameters in the raw waveform processing step (2 choices<sup>1</sup>), distance transformations (3 choices<sup>2</sup>), distance metric (5 choices<sup>3</sup>) and linkage type (4 choices<sup>4</sup>), we obtain 120 different trees, one for each combination of parameters.

## 4.3. Implementation of C-FAR

Each of the original hierarchical clustering tree was first converted into a tree object instance of a customized MATLAB tree class adopted from (Tinevez, 2020). Each node of this first tree (named composition tree) stores a list of unit IDs clustered at this node. A second tree (named purity tree) whose structure is synchronized with the first tree, stores the purity value (whether the clustering defined by this node in the corresponding composition tree is correct, wrong, or unknown) in each node.<sup>5</sup> Next, ground truth cluster labels was converted into a pairwise ground truth decision matrix indicting whether any given two pairs of unit belongs to the same cluster. After that, `FindOneBlock` was initialized with a leaf node (pure by definition) and executed through repeatedly asking users ( or in this case, the ground truth decision matrix ) the purity of some nodes. Before the next query, all past answers obtained were consulted first to see if the answer to the current question could already be inferred before consulting ground truth matrix or users. Whenever an impure node is identified at any step, the purity of all nodes inside the forest whose composition is a super set of that of the impure node is updated as impure simultaneously so their purity will not be queried for user feedback again. At the end of `FindOneBlock` when one block of true clusters was found. Units forming this block would then be appended to the clustering result, eliminated from all trees before `FindOneBlock` was executed for another iteration until all forest became empty. Between iterations, purity trees were reinitialized with to be the state unknown.

## 4.4. Evaluation and results

Dateset was generated on Linus OS (Ubuntu 18.04) using the command line interface provided (Buccino & Einevoll, 2019). Hierarchical clustering as well as C-FAR were performed with Matlab 2017a running on a Windows 10 computer equipped with 16-core Intel Xeon E5-2670 CPU. Converting from original hierarchical clustering result returned

<sup>1</sup>raw or take first derivative in time for each channel

<sup>2</sup>none, first ten PCA components across units or first 3 components of tSNE across units

<sup>3</sup>Euclidean, squared Euclidean, Manhattan, Chebychev or correlation

<sup>4</sup>single, average, complete, weighted

<sup>5</sup>For speed improvements, the forest formed by all composition trees was further converted into a 3D boolean array of shape (number of nodes)-by-(number of units)-by-(number of trees) through one hot encoding of unit IDs

by MATLAB function `linkage()` into the C-FAR ready data structure was performed with 8-core parallel computation with using MATLAB parallel computing toolbox. Performance metrics for accuracy are the number of clusters (cf. Figure 1, top) and adjusted mutual information (AMI) between true and inferred labels (Vinh et al., 2010; 2009) (cf. Figure 5). Figure 1 (bottom) shows the run time in seconds, while Figure 5 (bottom) shows the average number of queries (number of pairwise comparisons) a user must provide for the algorithm to outputs a clustering based on the given trees. For one tree, (Gentile et al., 2019) showed that the number of queries is  $O(n)$  where  $n$  is the number of leaves of the tree. Thus our experimental results show that the number of queries of C-FAR scales as  $\log(n) + \log(m)$ , where  $m$  is the number of input trees and  $n$  is the initial number of clusters (cf. Figure 5).

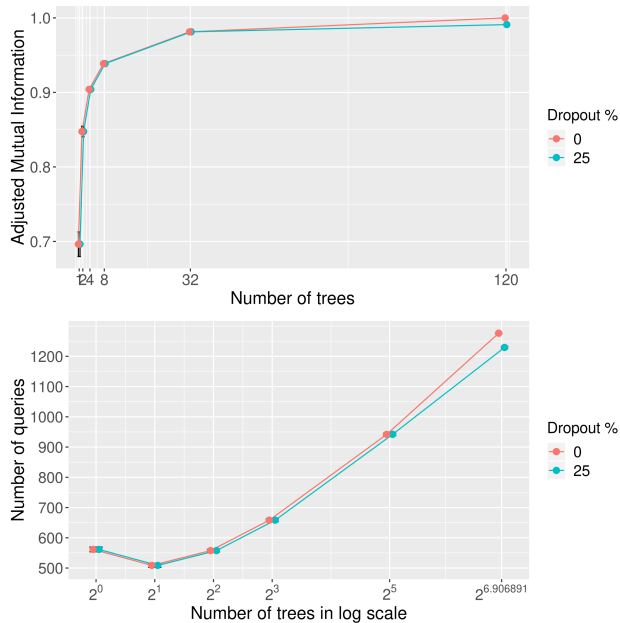


Figure 5. Additional performance metrics for C-FAR on our dataset. **Top.** adjusted mutual information (AMI) between the true and the cluster estimated by the algorithm vs number of input trees. An AMI of 1 means the estimated clusters are equal to the true; higher number means better performance. **Bottom** Number of queries (bottom) vs number of input trees in log scale. From the one-tree algorithm of (Gentile et al., 2019) to just using 8 trees in C-FAR, adjusted mutual information increases sharply while the average number of queries only increase by 17% (from 561 to 658)

As seen from Figures 1 and 5, the C-FAR algorithm has significantly better accuracy over the original one-tree algorithm of (Gentile et al., 2019) while paying little in computation penalty. The average number of clusters drops from more than twice the true number with one tree to within

10% of the true with 8 trees (cf. Figure 1), while adjusted mutual information climbs from 0.7 to 0.94. In addition, the number of queries of C-FAR scales as  $\log(m)$  (cf. Figure 5), with total runtime scales linearly in  $m$  (cf. Figure 1).

#### 4.5. Summary

This paper presents C-FAR, an ensemble clustering algorithm that takes in an arbitrary number of hierarchical clustering trees, prompts the user for pairwise comparisons between strategically chosen pairs of clusters, and outputs a flattened clustering. It generalizes the one-tree algorithm of (Gentile et al., 2019). By taking advantage of the common information across multiple trees, our algorithm performs significantly better than the one-tree case in simulated neuroscience data, with only a linear increase in total computation time. These results indicate that C-FAR is highly suitable as a model selection and assessment tool in clustering tasks, especially in the spike-sorting problem in neuroscience.

#### References

- Ailon, N., Bhattacharya, A., Jaiswal, R., and Kumar, A. Approximate clustering with same-cluster queries. *arXiv preprint arXiv:1704.01862*, 2017.
- Alqurashi, T. and Wang, W. Clustering ensemble method. *International Journal of Machine Learning and Cybernetics*, 10(6):1227–1246, 2019.
- Ashtiani, H., Kushagra, S., and Ben-David, S. Clustering with same-cluster queries. In *Advances in neural information processing systems*, pp. 3216–3224, 2016.
- Awasthi, P., Balcan, M. F., and Voevodski, K. Local algorithms for interactive clustering. *The Journal of Machine Learning Research*, 18(1):75–109, 2017.
- Ayad, H. G. and Kamel, M. S. On voting-based consensus of cluster ensembles. *Pattern Recognition*, 43(5):1943–1953, 2010.
- Balcan, M.-F. and Blum, A. Clustering with interactive feedback. In *International Conference on Algorithmic Learning Theory*, pp. 316–328. Springer, 2008.
- Barrese, J. C., Rao, N., Paroo, K., Triebwasser, C., Vargas-Irwin, C., Franquemont, L., and Donoghue, J. P. Failure mode analysis of silicon-based intracortical microelectrode arrays in non-human primates. *Journal of neural engineering*, 10(6):066014, 2013.
- Blanche, T. J., Spacek, M. A., Hetke, J. F., and Swindale, N. V. Polytrodes: high-density silicon electrode arrays for large-scale multiunit recording. *Journal of neurophysiology*, 93(5):2987–3000, 2005.

- Buccino, A. P. and Einevoll, G. T. Mearec: a fast and customizable testbench simulator for ground-truth extracellular spiking activity. *bioRxiv*, 2019. doi: 10.1101/691642. URL <https://www.biorxiv.org/content/early/2019/07/03/691642>.
- Calabrese, A. and Paninski, L. Kalman filter mixture model for spike sorting of non-stationary data. *Journal of neuroscience methods*, 196(1):159–169, 2011.
- Campbell, C., Cristianini, N., Smola, A., et al. Query learning with large margin classifiers. In *ICML*, volume 20, pp. 0, 2000.
- Cao, N., Gotz, D., Sun, J., and Qu, H. Dicon: Interactive visual analysis of multidimensional clusters. *IEEE transactions on visualization and computer graphics*, 17(12):2581–2590, 2011.
- Carlson, D. E., Vogelstein, J. T., Wu, Q., Lian, W., Zhou, M., Stoetzner, C. R., Kipke, D., Weber, D., Dunson, D. B., and Carin, L. Multichannel electrophysiological spike sorting via joint dictionary learning and mixture modeling. *IEEE Transactions on Biomedical Engineering*, 61(1):41–54, 2013.
- Cavallo, M. and Demiralp, Ç. Clustrophile 2: guided visual clustering analysis. *IEEE transactions on visualization and computer graphics*, 25(1):267–276, 2018.
- Chatziafratis, V., Niazadeh, R., and Charikar, M. Hierarchical clustering with structural constraints. *arXiv preprint arXiv:1805.09476*, 2018.
- Chen, Y., Jalali, A., Sanghavi, S., and Xu, H. Clustering partially observed graphs via convex optimization. *The Journal of Machine Learning Research*, 15(1):2213–2238, 2014.
- Chung, J. E., Magland, J. F., Barnett, A. H., Tolosa, V. M., Tooker, A. C., Lee, K. Y., Shah, K. G., Felix, S. H., Frank, L. M., and Greengard, L. F. A fully automated approach to spike sorting. *Neuron*, 95(6):1381–1394, 2017.
- Chung, J. E., Joo, H. R., Fan, J. L., Liu, D. F., Barnett, A. H., Chen, S., Geaghan-Breiner, C., Karlsson, M. P., Karlsson, M., Lee, K. Y., et al. High-density, long-lasting, and multi-region electrophysiological recordings using polymer electrode arrays. *Neuron*, 101(1):21–31, 2019.
- Dasarathy, G., Nowak, R., and Zhu, X. S2: An efficient graph based active learning algorithm with application to nonparametric classification. In *Conference on Learning Theory*, pp. 503–522, 2015.
- Dasgupta, S. and Hsu, D. Hierarchical sampling for active learning. In *Proceedings of the 25th international conference on Machine learning*, pp. 208–215. ACM, 2008.
- Dhawale, A. K., Poddar, R., Wolff, S. B., Normand, V. A., Kopelowitz, E., and Ölveczky, B. P. Automated long-term recording and analysis of neural activity in behaving animals. *Elife*, 6:e27702, 2017.
- Dudoit, S. and Fridlyand, J. Bagging to improve the accuracy of a clustering procedure. *Bioinformatics*, 19(9):1090–1099, 2003.
- Eriksson, B., Dasarathy, G., Singh, A., and Nowak, R. Active clustering: Robust and efficient hierarchical clustering using adaptively selected similarities. In *Proceedings of the Fourteenth International Conference on Artificial Intelligence and Statistics*, pp. 260–268, 2011.
- Fern, X. Z. and Brodley, C. E. Random projection for high dimensional data clustering: A cluster ensemble approach. In *Proceedings of the 20th international conference on machine learning (ICML-03)*, pp. 186–193, 2003.
- Fern, X. Z. and Brodley, C. E. Solving cluster ensemble problems by bipartite graph partitioning. In *Proceedings of the twenty-first international conference on Machine learning*, pp. 36. ACM, 2004.
- Fred, A. L. and Jain, A. K. Combining multiple clusterings using evidence accumulation. *IEEE transactions on pattern analysis and machine intelligence*, 27(6):835–850, 2005.
- Gentile, C., Vitale, F., and Rajagopalan, A. Flattening a hierarchical clustering through active learning. *arXiv preprint arXiv:1906.09458*, 2019.
- Gilletti, A. and Muthuswamy, J. Brain micromotion around implants in the rodent somatosensory cortex. *Journal of neural engineering*, 3(3):189, 2006.
- Gionis, A., Mannila, H., and Tsaparas, P. Clustering aggregation. *ACM Transactions on Knowledge Discovery from Data (TKDD)*, 1(1):4, 2007.
- Gokhale, C., Das, S., Doan, A., Naughton, J. F., Rampalli, N., Shavlik, J., and Zhu, X. Corleone: hands-off crowdsourcing for entity matching. In *Proceedings of the 2014 ACM SIGMOD international conference on Management of data*, pp. 601–612. ACM, 2014.
- Harris, K. D., Hirase, H., Leinekugel, X., Henze, D. A., and Buzsáki, G. Temporal interaction between single spikes and complex spike bursts in hippocampal pyramidal cells. *Neuron*, 32(1):141–149, 2001.
- Hofmann, T. and Buhmann, J. M. Active data clustering. In *Advances in Neural Information Processing Systems*, pp. 528–534, 1998.



- Hong, G. and Lieber, C. M. Novel electrode technologies for neural recordings. *Nature Reviews Neuroscience*, pp. 1, 2019.
- Huang, D., Lai, J.-H., and Wang, C.-D. Robust ensemble clustering using probability trajectories. *IEEE transactions on knowledge and data engineering*, 28(5):1312–1326, 2015.
- Huang, R. and Lam, W. Semi-supervised document clustering via active learning with pairwise constraints. In *Seventh IEEE International Conference on Data Mining (ICDM 2007)*, pp. 517–522. IEEE, 2007.
- Hurwitz, C., Xu, K., Srivastava, A., Buccino, A., and Hennig, M. Scalable spike source localization in extracellular recordings using amortized variational inference. In Wallach, H., Larochelle, H., Beygelzimer, A., d Alché-Buc, F., Fox, E., and Garnett, R. (eds.), *Advances in Neural Information Processing Systems 32*, pp. 4726–4738. Curran Associates, Inc., 2019.
- Iam-On, N., Boongoen, T., Garrett, S., and Price, C. A link-based approach to the cluster ensemble problem. *IEEE transactions on pattern analysis and machine intelligence*, 33(12):2396–2409, 2011.
- Karypis, G. and Kumar, V. A fast and high quality multilevel scheme for partitioning irregular graphs. *SIAM Journal on scientific Computing*, 20(1):359–392, 1998.
- Krishnamurthy, A., Balakrishnan, S., Xu, M., and Singh, A. Efficient active algorithms for hierarchical clustering. *arXiv preprint arXiv:1206.4672*, 2012.
- Lewis, D. D. and Gale, W. A. A sequential algorithm for training text classifiers. In *SIGIR94*, pp. 3–12. Springer, 1994.
- Lex, A., Streit, M., Partl, C., Kashofer, K., and Schmalstieg, D. Comparative analysis of multidimensional, quantitative data. *IEEE Transactions on Visualization and Computer Graphics*, 16(6):1027–1035, 2010.
- Lex, A., Streit, M., Schulz, H.-J., Partl, C., Schmalstieg, D., Park, P. J., and Gehlenborg, N. Stratomex: visual analysis of large-scale heterogeneous genomics data for cancer subtype characterization. In *Computer graphics forum*, volume 31, pp. 1175–1184. Wiley Online Library, 2012.
- Li, Y., Tang, S., and de Sa, V. R. Supervised spike sorting using deep convolutional siamese network and hierarchical clustering. unpublished thesis, 2019.
- Lipor, J. and Balzano, L. Leveraging union of subspace structure to improve constrained clustering. In *Proceedings of the 34th International Conference on Machine Learning-Volume 70*, pp. 2130–2139. JMLR. org, 2017.
- Luan, L., Wei, X., Zhao, Z., Siegel, J. J., Potnis, O., Tuppen, C. A., Lin, S., Kazmi, S., Fowler, R. A., Holloway, S., et al. Ultraflexible nanoelectronic probes form reliable, glial scar-free neural integration. *Science Advances*, 3(2):e1601966, 2017.
- L’Yi, S., Ko, B., Shin, D., Cho, Y.-J., Lee, J., Kim, B., and Seo, J. Xclusim: a visual analytics tool for interactively comparing multiple clustering results of bioinformatics data. *BMC bioinformatics*, 16(11):S5, 2015.
- Mallapragada, P. K., Jin, R., and Jain, A. K. Active query selection for semi-supervised clustering. In *2008 19th International Conference on Pattern Recognition*, pp. 1–4. IEEE, 2008.
- Mazumdar, A. and Saha, B. Clustering with noisy queries. In *Advances in Neural Information Processing Systems*, pp. 5788–5799, 2017a.
- Mazumdar, A. and Saha, B. A theoretical analysis of first heuristics of crowdsourced entity resolution. In *Thirty-First AAAI Conference on Artificial Intelligence*, 2017b.
- Mimaroglu, S. and Aksehirli, E. Diclens: Divisive clustering ensemble with automatic cluster number. *IEEE/ACM transactions on computational biology and bioinformatics*, 9(2):408–420, 2011.
- Monti, S., Tamayo, P., Mesirov, J., and Golub, T. Consensus clustering: a resampling-based method for class discovery and visualization of gene expression microarray data. *Machine learning*, 52(1-2):91–118, 2003.
- Nam, E. J., Han, Y., Mueller, K., Zelenyuk, A., and Imre, D. Clustersculptor: A visual analytics tool for high-dimensional data. In *2007 IEEE Symposium on Visual Analytics Science and Technology*, pp. 75–82. IEEE, 2007.
- Nguyen, H. T. and Smeulders, A. Active learning using pre-clustering. In *Proceedings of the twenty-first international conference on Machine learning*, pp. 79. ACM, 2004.
- Pachitariu, M., Steinmetz, N. A., Kadir, S. N., Carandini, M., and Harris, K. D. Fast and accurate spike sorting of high-channel count probes with kilosort. In *Advances in Neural Information Processing Systems*, pp. 4448–4456, 2016.
- Pachitariu, M., Stringer, C., Steinmetz, N., Carandini, M., and Harris, K. Drift correction for electrophysiology and two-photon calcium imaging. 3 2018. doi: 10.25378/janelia.5946574.v1. URL [https://janelia.figshare.com/articles/Drift\\_correction\\_for\\_electrophysiology\\_and\\_two-photon\\_calcium\\_imaging/5946574](https://janelia.figshare.com/articles/Drift_correction_for_electrophysiology_and_two-photon_calcium_imaging/5946574).

- Pilhöfer, A., Gribov, A., and Unwin, A. Comparing clusterings using bertin's idea. *IEEE Transactions on Visualization and Computer Graphics*, 18(12):2506–2515, 2012.
- Quirk, M. C., Blum, K. I., and Wilson, M. A. Experience-dependent changes in extracellular spike amplitude may reflect regulation of dendritic action potential back-propagation in rat hippocampal pyramidal cells. *Journal of Neuroscience*, 21(1):240–248, 2001.
- Ramaswamy, S., Courcol, J.-D., Abdellah, M., Adaszewski, S. R., Antille, N., Arsever, S., Atenekeng, G., Bilgili, A., Brukau, Y., Chalimourda, A., et al. The neocortical microcircuit collaboration portal: a resource for rat somatosensory cortex. *Frontiers in neural circuits*, 9:44, 2015.
- Rodriguez, A. and Laio, A. Clustering by fast search and find of density peaks. *Science*, 344(6191):1492–1496, 2014.
- Rossant, C., Kadir, S. N., Goodman, D. F., Schulman, J., Hunter, M. L., Saleem, A. B., Grosmark, A., Belluscio, M., Denfield, G. H., Ecker, A. S., et al. Spike sorting for large, dense electrode arrays. *Nature neuroscience*, 19(4):634, 2016.
- Rousche, P. J. and Normann, R. A. A method for pneumatically inserting an array of penetrating electrodes into cortical tissue. *Annals of biomedical engineering*, 20(4):413–422, 1992.
- Sacha, D., Kraus, M., Bernard, J., Behrisch, M., Schreck, T., Asano, Y., and Keim, D. A. Somflow: Guided exploratory cluster analysis with self-organizing maps and analytic provenance. *IEEE transactions on visualization and computer graphics*, 24(1):120–130, 2017.
- Schreck, T., Bernard, J., Von Landesberger, T., and Kohlhammer, J. Visual cluster analysis of trajectory data with interactive kohonen maps. *Information Visualization*, 8(1):14–29, 2009.
- Schütze, H., Velipasaoğlu, E., and Pedersen, J. O. Performance thresholding in practical text classification. In *Proceedings of the 15th ACM international conference on Information and knowledge management*, pp. 662–671. ACM, 2006.
- Seo, J. and Shneiderman, B. Interactively exploring hierarchical clustering results [gene identification]. *Computer*, 35(7):80–86, 2002.
- Shamir, O. and Tishby, N. Spectral clustering on a budget. In *Proceedings of the Fourteenth International Conference on Artificial Intelligence and Statistics*, pp. 661–669, 2011.
- Song, A. H., Flores, F., and Ba, D. Spike sorting by convolutional dictionary learning. *arXiv preprint arXiv:1806.01979*, 2018.
- Strehl, A. and Ghosh, J. Cluster ensembles—a knowledge reuse framework for combining multiple partitions. *Journal of machine learning research*, 3(Dec):583–617, 2002.
- Subbaroyan, J., Martin, D. C., and Kipke, D. R. A finite-element model of the mechanical effects of implantable microelectrodes in the cerebral cortex. *Journal of neural engineering*, 2(4):103, 2005.
- Szarowski, D., Andersen, M., Retterer, S., Spence, A., Isaacson, M., Craighead, H., Turner, J., and Shain, W. Brain responses to micro-machined silicon devices. *Brain research*, 983(1-2):23–35, 2003.
- Takahashi, S., Sakurai, Y., Tsukada, M., and Anzai, Y. Classification of neuronal activities from tetrode recordings using independent component analysis. *Neurocomputing*, 49(1-4):289–298, 2002.
- Takekawa, T., Isomura, Y., and Fukai, T. Spike sorting of heterogeneous neuron types by multimodality-weighted pca and explicit robust variational bayes. *Frontiers in neuroinformatics*, 6:5, 2012.
- Tinevez, J.-Y. Tree data structure as a matlab class, 2020. URL <https://www.github.com/tinevez/matlab-tree>.
- Tong, S. and Chang, E. Support vector machine active learning for image retrieval. In *Proceedings of the ninth ACM international conference on Multimedia*, pp. 107–118. ACM, 2001.
- Vega-Pons, S. and Ruiz-Shulcloper, J. A survey of clustering ensemble algorithms. *International Journal of Pattern Recognition and Artificial Intelligence*, 25(03):337–372, 2011.
- Vesdapunt, N., Bellare, K., and Dalvi, N. Crowdsourcing algorithms for entity resolution. *Proceedings of the VLDB Endowment*, 7(12):1071–1082, 2014.
- Vinh, N. X., Epps, J., and Bailey, J. Information theoretic measures for clusterings comparison: is a correction for chance necessary? In *Proceedings of the 26th annual international conference on machine learning*, pp. 1073–1080, 2009.
- Vinh, N. X., Epps, J., and Bailey, J. Information theoretic measures for clusterings comparison: Variants, properties, normalization and correction for chance. *Journal of Machine Learning Research*, 11(Oct):2837–2854, 2010.

- Voiron, N., Benoit, A., Lambert, P., and Ionescu, B. Deep learning vs spectral clustering into an active clustering with pairwise constraints propagation. In *2016 14th international workshop on content-based multimedia indexing (CBMI)*, pp. 1–6. IEEE, 2016.
- Wang, J., Kraska, T., Franklin, M. J., and Feng, J. Crowder: Crowdsourcing entity resolution. *Proceedings of the VLDB Endowment*, 5(11):1483–1494, 2012.
- Wang, L., Leckie, C., Kotagiri, R., and Bezdek, J. Approximate pairwise clustering for large data sets via sampling plus extension. *Pattern Recognition*, 44(2):222–235, 2011.
- Wauthier, F. L., Jojic, N., and Jordan, M. I. Active spectral clustering via iterative uncertainty reduction. In *Proceedings of the 18th ACM SIGKDD international conference on Knowledge discovery and data mining*, pp. 1339–1347. ACM, 2012.
- Wiwie, C., Baumbach, J., and Röttger, R. Comparing the performance of biomedical clustering methods. *Nature methods*, 12(11):1033, 2015.
- Xiong, C., Johnson, D. M., and Corso, J. J. Online active constraint selection for semi-supervised clustering. In *ECAI 2012 AIL Workshop*, 2012.
- Xiong, C., Johnson, D. M., and Corso, J. J. Active clustering with model-based uncertainty reduction. *IEEE transactions on pattern analysis and machine intelligence*, 39(1): 5–17, 2016.
- Xu, Z., Yu, K., Tresp, V., Xu, X., and Wang, J. Representative sampling for text classification using support vector machines. *Advances in Information Retrieval: 25th European Conf on IR Research ECIR 2003: 2003; Italy*, 2633: 11–11, 04 2003. doi: 10.1007/3-540-36618-0\_28.
- Yger, P., Spampinato, G. L., Esposito, E., Lefebvre, B., Deny, S., Gardella, C., Stimberg, M., Jetter, F., Zeck, G., Picaud, S., et al. Fast and accurate spike sorting in vitro and in vivo for up to thousands of electrodes. *BioRxiv*, pp. 067843, 2016.
- Yger, P., Spampinato, G. L., Esposito, E., Lefebvre, B., Deny, S., Gardella, C., Stimberg, M., Jetter, F., Zeck, G., Picaud, S., et al. A spike sorting toolbox for up to thousands of electrodes validated with ground truth recordings in vitro and in vivo. *Elife*, 7:e34518, 2018.
- Zhao, Z., Luan, L., Wei, X., Zhu, H., Li, X., Lin, S., Siegel, J. J., Chitwood, R. A., and Xie, C. Nanoelectronic coating enabled versatile multifunctional neural probes. *Nano letters*, 17(8):4588–4595, 2017.
- Zhou, J., Konecni, S., and Grinstein, G. Visually comparing multiple partitions of data with applications to clustering. In *Visualization and Data Analysis 2009*, volume 7243, pp. 72430J. International Society for Optics and Photonics, 2009.